Ain Shams Engineering Journal 10 (2019) 253–265

Contents lists available at ScienceDirect

Ain Shams Engineering Journal

journal homepage: www.sciencedirect.com

Mechanical Engineering

Observations of changes in acoustic emission parameters for varying corrosion defect in reciprocating compressor valves

Salah M. Ali [a,*], K.H. Hui [a], L.M. Hee [a], M. Salman Leong [a], Ahmed M. Abdelrhman [b], Mahdi A. Al-Obaidi [c]

[a] Institute of Noise and Vibration, University Technology Malaysia, 54100 Kuala Lumpur, Malaysia
[b] School of Engineering, Bahrain Polytechnic, 33349 Isa Town, Bahrain
[c] Energy and Renewable Energies Technology Center, University of Technology, 10001 Baghdad, Iraq

ARTICLE INFO

Article history:
Received 5 December 2016
Revised 7 January 2018
Accepted 1 January 2019
Available online 14 February 2019

Keywords:
Reciprocating compressor
Valve fault detection
Acoustic emission parameters
MANOVA
Coefficient of variance

ABSTRACT

Acoustic Emission (AE) technology is probably one of the most recent entries in the field of machinery condition monitoring. This paper investigates the application of AE parameters for valve faults detection in reciprocating compressor. The defective valves were designed by emulating the actual valve corrosion with varying sizes such that defects could be applied onto the reciprocating compressor. A set of experiments was performed to acquire the AE signal. The primary source of AE signal was verified using waveform analysis. The AE parameters versus different operational and valve condition were illustrated individually. In addition, the significance of the change and sensitivity of AE parameters versus different experimental conditions was verified using MANOVA and coefficient of variance analysis. It is concluded that the AE signal parameters can be used to detect the valve faults in the reciprocating compressor with the consideration of the variation in the AE parameters sensitivity.

1. Introduction

Reciprocating compressor is the most popular classes of machine used with wide applications in industry and it is considered the patriarch of the compressors family [1]. However, the unpredicted failures in this category of machine often result in dire consequences. Several industry surveys have cited valve faults as the most common cause for unplanned shutdown of reciprocating compressors [2,3]. Many defects have been found in the compressor valve, such as a clogged defect, a broken valve, a crack defect and corrosion. Therefore, an effective and accurate valve condition monitoring and fault diagnosis tool is extremely necessary to ensure maximum productivity and safe compressor operation.

The AE is a rapidly growing technique in the field of machinery condition monitoring and fault diagnosis due to the unique features of the AE which can supply valuable information about the energy sources inside the machine. The AE technology has been studied and reviewed by many researchers [4–7]. Acoustic emission refers to the generation of transient elastic waves produced by a rapid release of energy from a localized source within and/or on the surface of a material according to the definition by the American Society for Testing and Materials (ASTM) [8]. In this paper, AE is defined as transient elastic waves produced by the impact of one surface to another in a reciprocating motion. In other words, AE is the transient elastic waves produced by the impingement of the reeds inside the valve with the upper and lower valve housing during the reciprocating compressor operation.

Many methods based on vibration, pressure and current signals and the AE technique have been investigated for condition monitoring of compressors; however, only a less efforts were found investigating the feasibility of AE signal parameters in valve condition monitoring. For example, Yih et al. [9] proposed a strategy for the classification of the faults of reciprocating compressor valves via the post-processing vibration signal using short-time Fourier transform and Wigner-Ville distribution. Valve faults were concluded to be difficult to differentiate using the presented strategy. Ahmed et al. [10] developed a valve fault detection model by using principal component analysis (PCA) for selecting the vibration feature in reciprocating compressor valves. Although valve faults were demonstrated to be detected using this model, the sources of the faults were not investigated. Another model for valve fault detection was proposed by Van et al. [11] that implemented a

* Corresponding author.
E-mail address: salah.obaidi@pioneers-group.com (S.M. Ali).
Peer review under responsibility of Ain Shams University.

Production and hosting by Elsevier

https://doi.org/10.1016/j.asej.2019.01.003
2090-4479/

new type of learning architecture called deep belief networks (DBNs) and a Teager-Kaiser energy operator on three acquired signals: vibration, pressure and current signals. The proposed approach with DBNs was found to improve the accuracy of valve fault identification. Elhaj et al. [12] developed a mathematical model of a two-stage reciprocating compressor based on instantaneous angular speed (IAS) and cylinder pressure waveforms for detection and identification of different valve faults. Indeed, the pressure measurements revealed a clear detection feature, but it is an intrusive measurement that is difficult to implement. On the contrary, the IAS features are not as obviously clear as those of pressure, but it is of direct relevance in condition monitoring because it can be obtained non-intrusively. Artificial neural networks, support vector machines and information entropy were used with the noise and vibration signals to classify the reciprocating compressor condition in other studies [13,14].

The viability of AE as a diagnostic and prognostic tool has reported in many studies [15–17]. For instance, the seed defect sizes on a rolling bearing have been estimated by establishing a relationship between the AE signal parameters and the defect size [18–20]. Seal and blade rubbing has been detected via on line monitoring using AE technology in power turbines [21,22]. El-Ghamry et al. [23] developed a statistical feature isolation technique for the diagnosis of faults in reciprocating machines using the AE signal. The technique was used to a selected time window for the AE signal to identify machine faults. It was concluded that this methodology could be applied to the monitoring of many types of reciprocating machines and deferent faults using a variety of sensor data. Valve leakage was detected during reciprocating compressor operation [24], and the valve leakage amount was estimated using AE signal [25]. Detection of valve clearance using AE technology was investigated by Elamin et al. [26], who found that AE is a powerful and reliable method of detection and diagnosis of diesel engines valve faults. Recently Yuefei et al. [3] presented a methodology for reciprocating compressor valve fault detection by integrating the AE signal with the simulated valve motion. However, limited operational conditions were used in the study.

The aim of this paper is to ascertain the applicability of AE main parameters (rise time, duration, counts to peak, count, maximum amplitude, ASL, energy and RMS) for detecting the corrosion defects of reciprocating compressor valves under different operational conditions, particularly as the former has been reported to be fraught with many challenges. The paper structure presented as follows. Section 1 reviews the state of the art the techniques used in valve fault detection and the shortcomings of the existing AE analysis methods. Section 2 briefly describes the AE parameters. Section 3 illustrates the test rig and the instrumentation that have been used in the experiments. Section 4 explains the experimental procedure. Section 5 illustrates the experiments results and discussion. Section 6 concludes the paper.

2. AE signal parameters

The AE signal can be classified as a transient signal (Hit), continuous signal, or mixed mode signal. An AE transient signal has definite starting and ending points and can easily stray from the background noise, whereas an AE continuous signal has various amplitudes and frequencies over time [27]. A mixed mode signal contains both transient and continuous signals. An acquired AE signal has special parameters that can describe the AE event. These parameters can be related to the machine condition; thus, the interpretations of the AE parameters are considered to be a good indicator of condition monitoring and fault diagnoses [28]. See Fig. 1. The main AE signal parameters are defined as below:

a. **AE Hit:** A signal that exceeds the threshold and causes a system to accumulate data.
b. **Amplitude:** The highest measured voltage in a waveform, which is directly related to the AE energy. The units of decibels (dB) or millivolts (mV) are often used to express the AE amplitude.
c. **Duration:** The period of time between the first and last threshold crossings by the AE signal. The duration is generally expressed in microseconds (μsec).
d. **Rise Time:** The time interval between the triggering time of the AE signal and the AE signal peak. Similar to the duration, the rise time is generally expressed in microseconds (μsec).

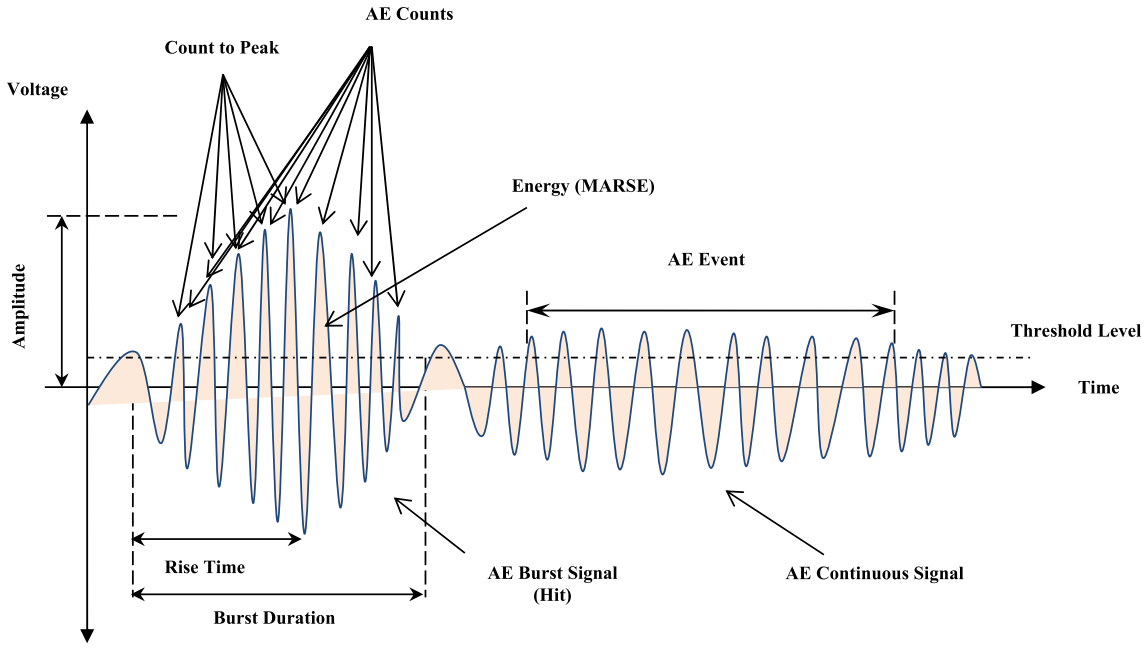

Fig. 1. The AE signal parameters.

e. **AE Counts:** The number of times where the signal exceeds a present threshold. The number of counts is also used to quantify the hits strength and the AE activity.
f. **Counts to Peak:** The number of counts between the triggering time over the threshold and the peak amplitude.
g. **RMS:** A statistical measure defined as the square root of the mean of the squares of the AE hits amplitude. The RMS of the AE hits amplitude is usually used because it is both unambiguous and has physical significance. RMS is usually measured on a linear scale and reported in volts, similar to the amplitude units.
h. **ASL:** A statistical measure defined as the average of the AE signal amplitude. Because the ASL considers the AE amplitude in a logarithmic scale, it must be reported in dB units.
i. **Energy:** The measured area under the rectified signal envelope (MARSE), with units that usually rely on the AE data acquisition method. In this paper, the energy is proportional to voltage and the duration of a signal (energy counts). However, energy is regularly used in the measurements of acoustic emissions due to its sensitivity to the amplitude as well as the duration.

3. Test rig and data acquisition system

A single stage, 2 cylinder, air-cooled industrial reciprocating air compressor (model: SWAN SVP-202) with a 1.5 kW/2 hp motor that can provide a maximum speed of 820 rpm was selected as a test rig in this study. A digital laser tachometer is configured and fixed near the test rig to receive a pulse from a piece of reflective tape attached to the flywheel to show the compressor cycle and to record the compressor speed. An AE sensor (model: PKWDI) with operating frequency range of 200–850 kHz was used to acquire the signal in this research. The sensor was placed at the valve/cylinder cover and fixed firmly to the surface by using super glue. A single-channel AE data acquisition system (model: USB AE Node) with AEwin™ software provides the full AE hit and time based features, including waveforms, was used to record AE signal and extract the AE parameters. The experiment setup is shown in Fig. 2.

Many threshold levels have been examined before acquiring the AE signal. The minimum values of thresholds were tested until the sensor began to detect the valve AE signals. Once the signal exceeded the setting threshold, the AE waveform was drafted versus the compressor cycle to ensure it represented the valve function (open-close). The signal was recognized perfectly at a threshold level of 55 db. A total of 2048 samples were recorded per acquisition (data file) at a sampling rates of 500 kHz.

4. Experimental procedure

The AE baseline signal (defect-free) was recorded for 12 running conditions: four speeds (200, 400, 600 and 800 rpm) and three flow rate conditions (0%, 50% and 100%). The speeds were controlled by the speed controller, while the flow rate was controlled by adjusting the amount of flow from the compressor outlet. The test configuration is described in Table 1.

Next, four valve conditions of varying corrosion severities were simulated on the discharge valve of the compressor. In an attempt to understand how the corrosion ratio influenced the AE parameters, an incremental procedure for simulating increasing corrosion ratio was established. Thus, the simulation of the corrosion ratio involved starting a sequence on a valve with simulation of a small corrosion with an oval shape and then increasing the area along the central direction of the valve reed until the maximum width was achieved in a similar manner as the actual defect of the corrosion. All the corrosion defects on the valve reed were simulated by removing from the reed material using a drilling machine. The corrosion defect severities are illustrated in Table 2 and Fig. 3.

Table 1
Test configuration.

Speed (RPM)		Flow rate (%)	
S1	200	F1	0%
S2	400	F2	50%
S3	600	F3	100%
S4	800		

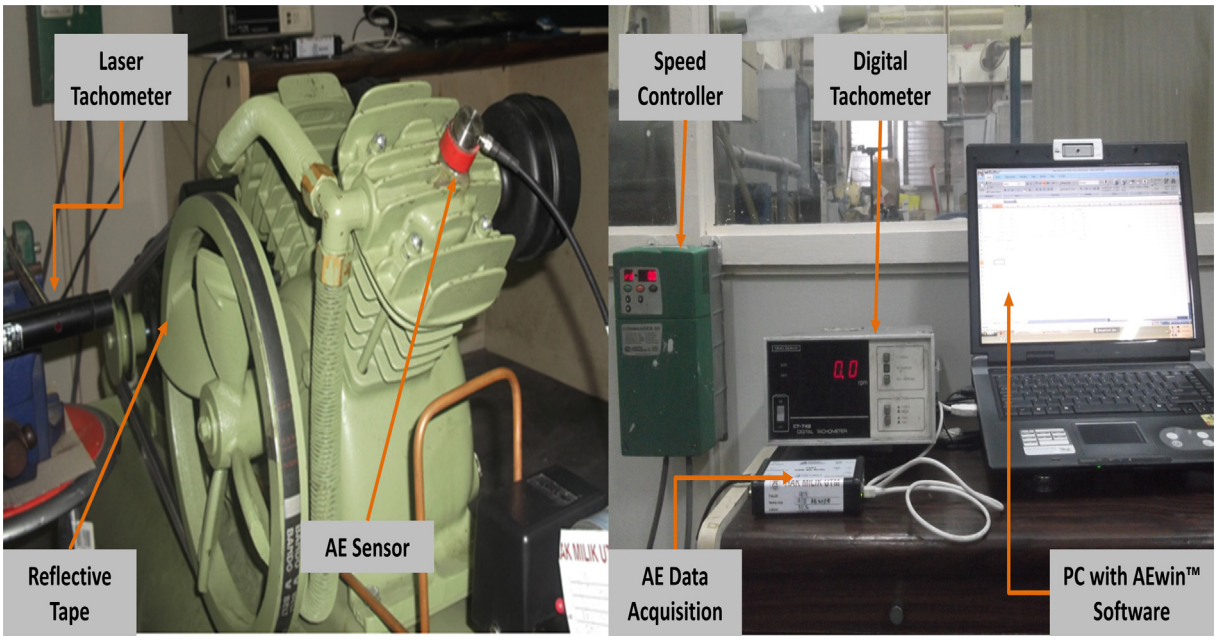

Fig. 2. Experimental test rig and data acquisition setup.

Table 2
Valve defects severities.

Valve condition	Defect type	Defect severity	Defect symbol	Defect size
Healthy Condition	No Defect	No Corrosion	NC	No defect
Faulty Condition	Corrosion Defect	Small Corrosion	SC	56.57 mm^2
		Medium Corrosion	MC	79.63 mm^2
		Large Corrosion	LC	106.27 mm^2
		Very Large Corrosion	VC	136.48 mm^2

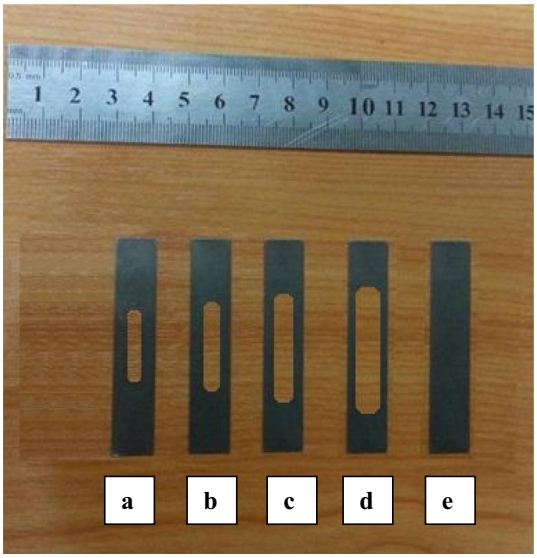

Fig. 3. The actual samples of valve's reed corrosion defect (a) SC, (b) MC, (c) LC, (d) VC and (e) NC.

For accuracy reasons, three sets of signal were acquired for each condition; the average values were calculated and taken as the final result (the average values of all AE parameters are detailed in Tables A1–A8 in Appendix A). A total of 180 experiments were performed for averaging the 12 conditions in this study, where each experiment was performed for 30 sec to acquire the AE signal. Experimental tests were performed by first producing the defects of the appropriate size and geometrical shape. After installing the faulty reeds inside the compressor discharge valve, the test rig was run at the first speed and flow rate condition. The test was repeated for 3 times, with the AE signal acquired for 30 sec in each condition. Next, the test rig was shutdown, and then the reed was replaced with another level of fault severity. Thus, the procedure for speed and flow rate was repeated, and then AE signal was again acquired. The AE parameters were extracted and collected for further analysis.

5. Results and discussion

5.1. Verification of the primary source of the AE signal

In particular, the suction and discharge process are the main two events for any reciprocating compressor in one operational cycle. In another word, when piston completed one cycle 360° from the cylinder top dead center coming back to the top dead center again, the valve plats will open and close respectively to allow the suction and discharge process. Consequently, as the valve plates bending up and down by the force of the piston pressure, the plate surface will impact the valve upper and lower part which made a rapid release of energy that generates strong transient elastic AE waves can detect by the AE sensor mounted on the valve/-cylinder cover. See Fig. 2.

Therefore, to verify the acquired AE signal is a consequence of the impact of the plates with the valve housing during the reciprocating compressor operation, the AE signal was recorded and plotted simultaneously with the compressor cycle in two conditions. First AE waveform was obtained from the acquired baseline signals which refer to the valve in healthy condition. The second waveform was acquired later after removing the discharge and suction valve's reeds. As stated before, both cases have been recorded with four speeds (200 rpm, 400 rpm, 600 rpm and 800 rpm) and one flow rate (100%).

In addition, if the reed's impacts were to produce the AE transient bursts, it was hypothesized that the AE hits would be detected at a rate equivalent to the valve movement frequency per cycle. Hence, the compressor valve must be open and closed within one cycle; two AE hits should appear per one compressor cycle representing the open and closed process. Moreover, it was hypothesized that the time between AE hits would be equivalent to the valve open-close timing, which can be obtained from the compressor speed. One operational cycle time can be calculated from the compressor speed as shown in Eq. (1) below:

$$OneCycleTime\ (\mathrm{Sec}) = \frac{1}{CrankShaftSpeed(\mathrm{RPM})} \times \tag{1}$$

Table 3 illustrates the actual speeds with the corresponding one cycle time calculated by the above equation. Thus, a plot includes both the tachometer signal and both AE waveforms have been plotted for every speed to verify the synchronization of the AE hits with the valve open and close events. Both tachometer signal and AE signal was drawn using FAMOS software. In all the four speeds, one second of the signal was segregated and analyzed. Figs. 4–7 illustrates two AE waveforms versus tachometer signal for each speed.

As it was perceived, AE waveform is directly associated with the valve function (open-close) as it clearly appears in all conditions. Transient type of AE waveform is dominant among the acquired AE signal in a sequence of bursts whose amplitude exceeds the underlying continuous wave whilst the hits find to be disappeared when the plates were removed from the valve. The frequency of the periodicity of the AE hits represented the valve movements (open-close) respectively within one cycle. This is similar to observations of AE waveforms associated with actual and simulated valve movement in reciprocating compressor which transient type forms of AE signal were apparently associated with the valve movement [3].

On the other hand, the time period between every (close-close) or (open-open) found to be the same time of one compressor cycle which found to be: 0.3 sec when the speed was 200 rpm, 0.15 sec

Table 3
The actual speeds with the corresponding 1 cycle time.

Experiments No	Speed (rpm)	Speed (rps)	Time of 1 Cycle (Sec)
1	200	3.33	0.30
2	400	6.67	0.15
3	600	10.00	0.10
4	800	13.33	0.075

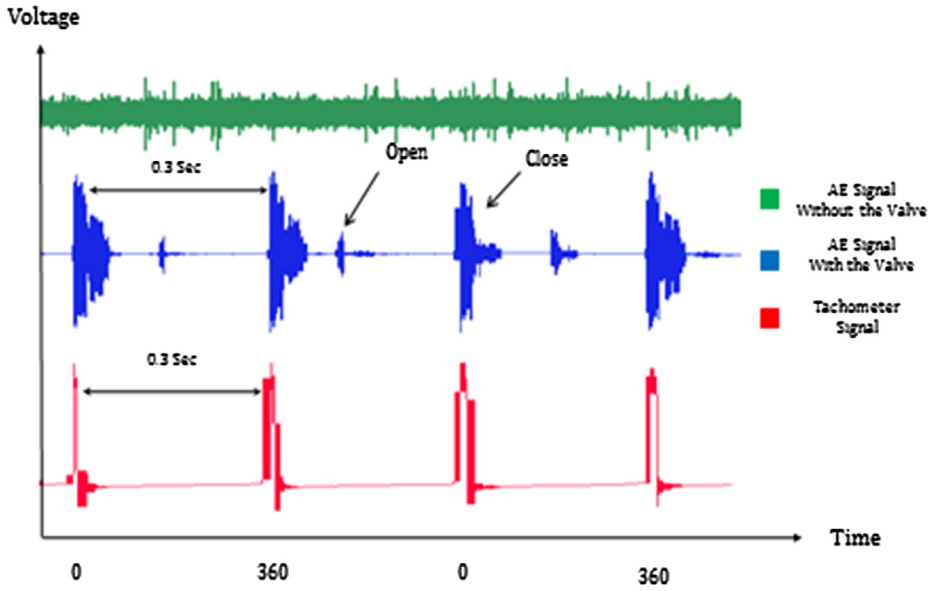

Fig. 4. AE waveforms versus compressor cycles at 200 rpm.

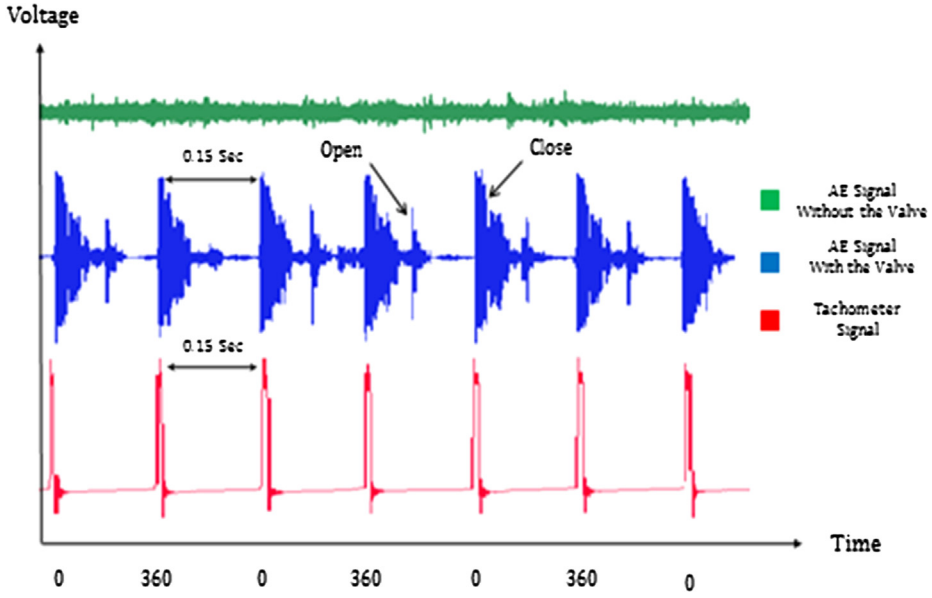

Fig. 5. AE waveforms versus compressor cycles at 400 rpm.

when the speed was 400 rpm, 0.09 sec when the speed was 600 rpm and 0.07 sec when the speed was 800 rpm. See Figs. 4–7 respectively. The time considers another indicator to prove that the hit signal was produced from the reed's impact with the valve housing.

5.2. Observation of AE parameters

5.2.1. AE rise time and duration

Rise time and duration are the time measurements used for the AE hits; both quantities represent the time period for one single hit, as mentioned previously. The rise time and duration values were compared under different valve corrosion defect ratios at varying speed and flow rate conditions. Note that the rise time values increase with the increase in the flow rate and speed for all conditions. The rise time values exhibit incremental decreases with the increase in the corrosion ratio for all speed and flow rate conditions (see Fig. 8). However, the rise time was found to be more sensitive for high speed rather than low speed for all corrosion ratios. For example, the rise time at SC, MC and VC conditions exhibited very small increases (3500–5000 μsec) with the increase in flow rate at the first speed (200 rpm), while the change was noted to be much greater, ranging from 60,000 μsec to 25,000 μSec) at higher speeds (600 rpm and 800 rpm) with the change in flow rate, such as for the NC, LC and VC conditions.

Similar to the rise time, the line graph clearly exhibits a dramatic increase in the AE hits duration when the flow rate and speed increase for each condition. However, the duration is observed to decline when the corrosion defects expand until it exhibits the lowest values for the very large corrosion condition VC. The decrease in the duration value is a result of the material removal from the valve reeds, which reduce the reed stiffness as well as the area of impact between the reeds and the valve housing, resulting in small values of the durations compared to the

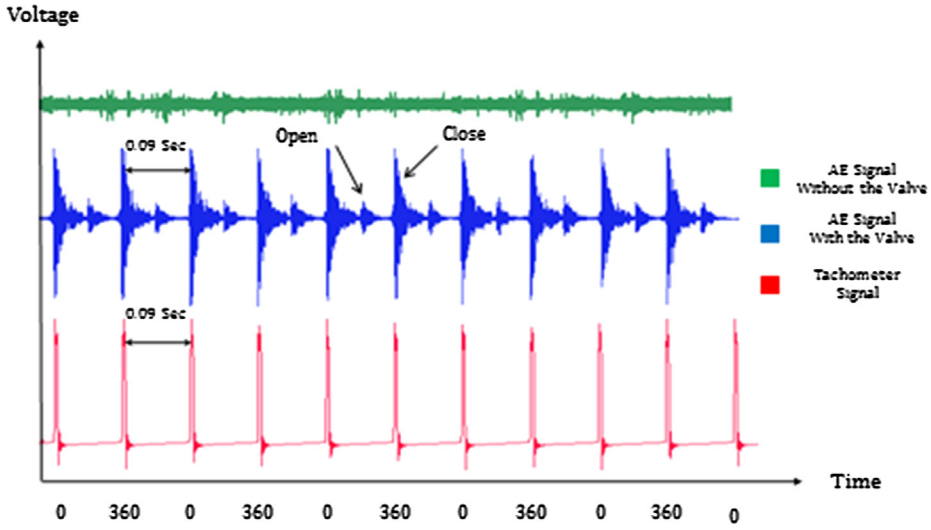

Fig. 6. AE waveforms versus compressor cycles at 600 rpm.

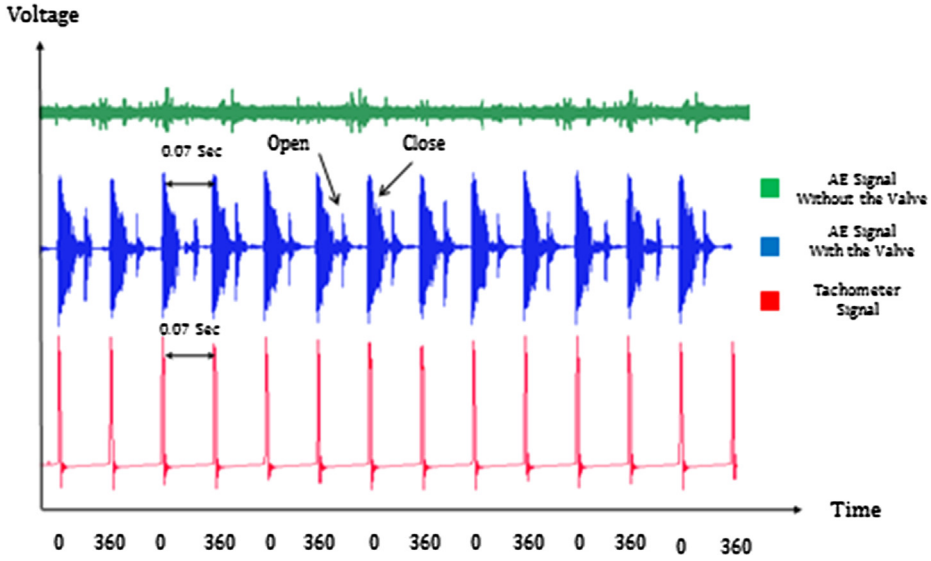

Fig. 7. AE waveforms versus compressor cycles at 800 rpm.

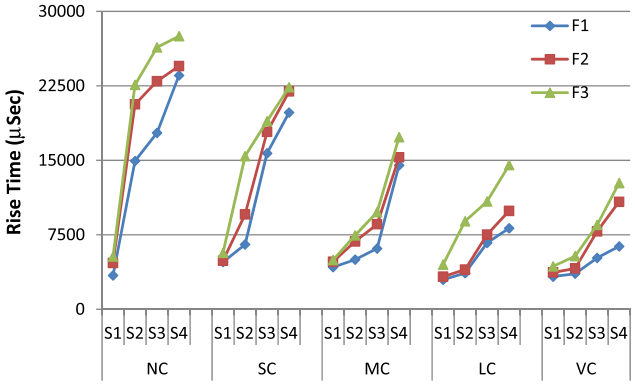

Fig. 8. AE rise time of different corrosion ratios at increasing speed and fix flow rate.

duration values when the valve is in the healthy condition. Nevertheless, the duration values show only small changes at the low speeds (12,000–14,000 µsec), while they show a huge difference when the speed increases (15,000 µsec up to 50,000 µsec). In addition, the duration noted was affected by the flow rate for nearly all conditions (except in the SC and VC) when the compressor ran at a low speed (see Fig. 9). The variation of the rise time and the duration values at increasing flow rate and fixed speed are detailed in Figs. B1 and B2 in Appendix B.

5.2.2. AE count to peak and counts

Counts and the count to peak are usually used to quantify the hits strength; they are proportional to each other because both represent the same hits. As the AE signal was recorded, the count and count to peak were calculated and obtained automatically via AEwin software for each single hit. Figs. 10 and 11 illustrate the counts and count to peak, respectively, for all test conditions. The line graphs in both figures show clear changes in both parameter values as the test conditions change. The values of counts to peak and counts were observed to be high at the healthy condition, followed by a decrease as the corrosion severity increases. The reason for this decrease is the volume of the material that was removed from the valve reeds, which lead to a decrease in the stiff-

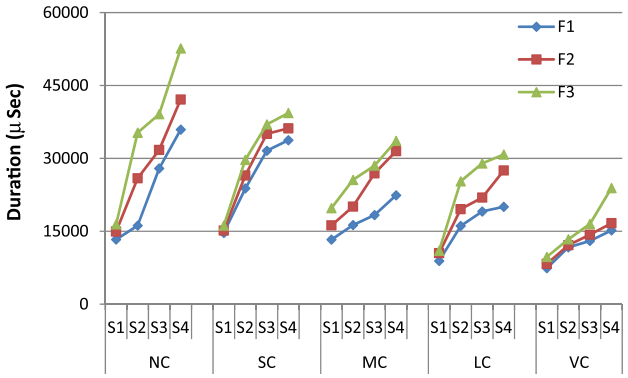

Fig. 9. AE duration of different corrosion ratios at increasing speed and fix flow rate.

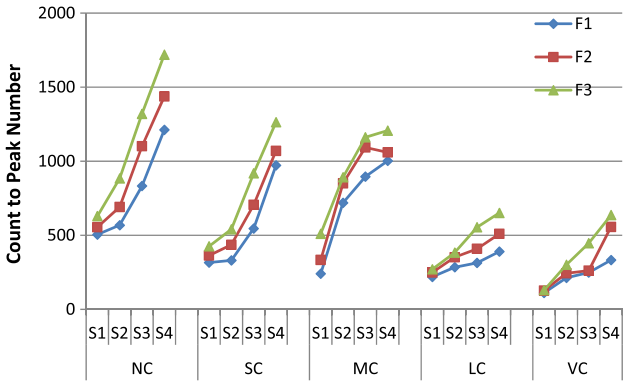

Fig. 10. AE count to peak of different corrosion ratios at increasing speed and fix flow rate.

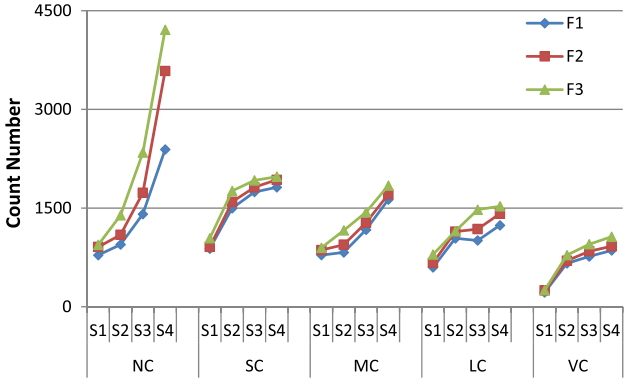

Fig. 11. AE count of different corrosion ratios at increasing speed and fix flow rate.

ness as well as in the impact area, which then lead to a reduction in the hits strength and result in a small number of counts and count to peak. For example, the AE count to peak for hits in the healthy condition was found to range from 500 counts up to 1700 counts and vary with the speed and the flow rate. As the speed increased from 200 rpm to 800 rpm, the count to peak increased accordingly. Moreover, the count-to-peak values were found to increase when the flow rate increased due to the decrease of the pressure inside the compressor (see Fig. 10).

The AE count number was found to have a similar behavior as the value of the count to peak, but with higher values. Thus, the count number values start to decline dramatically as the corrosion severity grows at the valve reeds. The count number ranged from 750 to 4500 counts at NC and then decreased from 300 to 750 counts at the VC, as shown in Fig. 11. This decline is again due to the removal of the material from the valve reed, which leads to a smaller number of counts because the stiffness and the area of contact become smaller. Comparable to the count to peak, the count number has identical behavior in terms of sensitivity to the flow rate and speed. Although the count number was found to be more sensitive to speed than flow rate, it still showed noticeable changes when the flow rate was changed at high speeds. However, the count number was difficult to differentiate in some conditions, especially at low speed, such as in the LC and VC conditions. The variation of the count and the count to peak values at increasing flow rate and fixed speed are detailed in Figs. B3 and B4 in Appendix B.

5.2.3. AE amplitude and ASL

The AE amplitude and AE average signal level were recorded and analyzed for all test conditions. Figs. 12 and 13 illustrate the results comparison of the AE amplitude and AE average signal levels, respectively. Both line graphs show a dramatic decrease in AE amplitude and ASL values with the increase in the corrosion severity. Because the reed material is removed gradually to simulate the corrosion defect, the stiffness as well as the contact area between the reeds and the valve housing were reduced, which influenced the AE hits strength; therefore, the AE amplitude and ASL were observed to decline with the increase in the corrosion severity. In addition, the AE amplitude and ASL were found to be more sensitive to the change in speed than the change in the flow rate. For example, the line graph clearly shows a spectacular increase in AE amplitude and ASL values with increasing speed in all test conditions. The maximum observation for amplitude was found to be (97 dB) at the first condition NC, while the lowest value was (86 dB) at the last condition, VC. The ASL value was observed to be maximum at the first condition (78 dB) and minimum (46 dB) at the LC condition. However, both AE amplitude and ASL values do not show a clear change with the increase in the flow rate. Both parameters showed comparable values with the change of flow rate. The variation of the AE amplitude and ASL values at increasing flow rate and fixed speed are detailed in Figs. B5 and B6 in Appendix B.

5.2.4. AE energy

AE energy is regularly used in the AE measurements to specify the overall cumulative AE event; therefore, AE energy was selected to compare different corrosion ratios at varying speed and flow rate conditions. In general, the energy values were found to decrease with the improvement of the corrosion in the valve reeds. The reason for this negative relation is related to the corrosion fault that was simulated into the valve reed as well as the nature of the

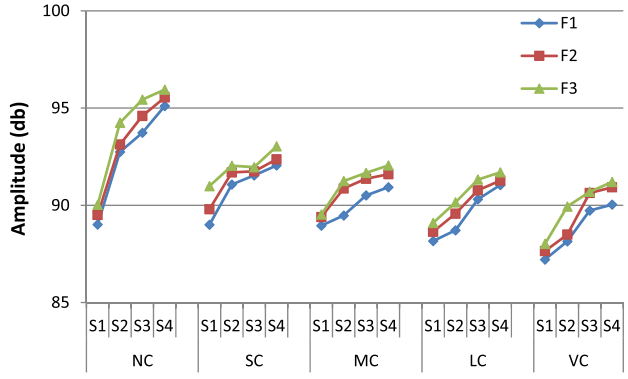

Fig. 12. AE amplitude of different corrosion ratios at increasing speed and fix flow rate.

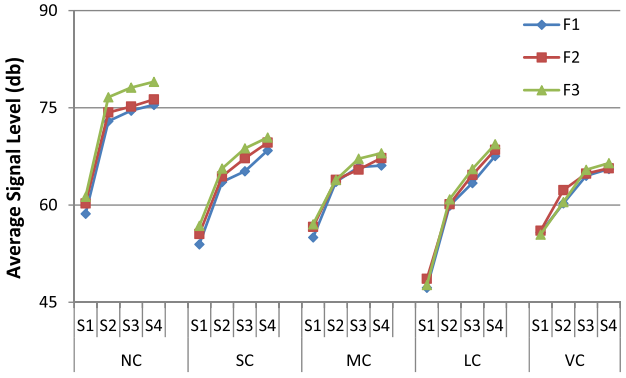

Fig. 13. AE ASL of different corrosion ratios at increasing speed and fix flow rate.

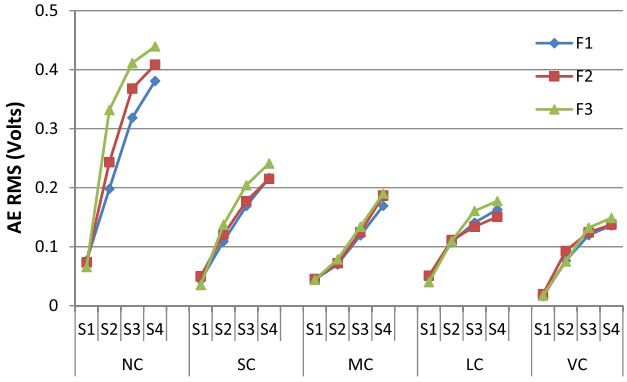

Fig. 15. AE RMS of different corrosion ratios at increasing speed and fix flow rate.

AE. As the main source of the AE events is correlated with the impact of the reeds with the valve housing, the strength of the AE event relies on the area of contact and the reed stiffness. Therefore, when the corrosion was gradually simulated into the valve reeds, the AE energy values decreased due to the removal of the material from the valve reed. Thus, the maximum energy was found to occur when the valve was in the healthy condition, NC, while the energy incrementally decreased until it reached the minimum value at the VC condition. However, the energy was observed to change with the change of flow rate and speed with a positive relationship, i.e., the energy values were found to increase with the increase in the flow rate and speed, as illustrated in Fig. 14. The variation of the energy values at increasing flow rate and fixed speed are detailed in Fig. B7 in Appendix B.

5.2.5. AE RMS

In general, the average power transmitted by an acoustic signal is proportional to the square of the root mean square of the AE hits amplitude. Therefore, the RMS of the AE hits amplitude was calculated, recorded and compared for all test conditions. Fig. 15 illustrates the changes of the RMS values by the change of the test conditions. As clearly shown in the line graph, the RMS values are found to decrease as the corrosion ratios increase. Among the five test conditions, the NC corresponds to the highest value of RMS (0.45 V), while the RMS was found to have the lowest values (0.02 V) at the VC condition. The reason for the decrease is the removal of the reed material, which resulted in reduction of the reed stiffness as well as the contact area between the reed and the valve housing, which negatively affects the AE amplitudes. Similar to the previous parameters, the RMS values were observed to increase with increasing flow rate for nearly all conditions, except at lower speeds, where the RMS values show small changes with the change of flow rate. Likewise, the RMS values were found to increase with the increase in the speed in all conditions. The RMS values were observed to be sensitive enough to detect the corrosion at high speeds (600 rpm and 800 rpm). The variation of the RMS values at increasing flow rate and fixed speed are detailed in Fig. B8 in Appendix B.

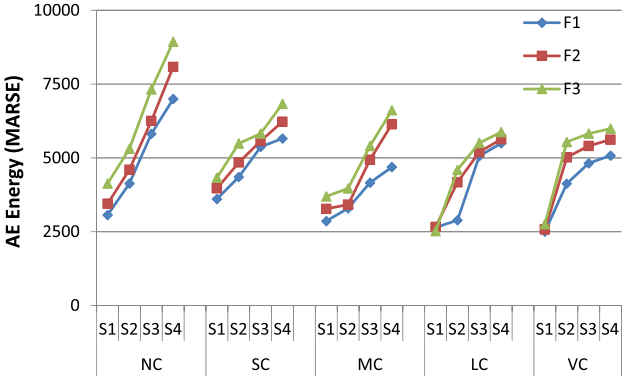

Fig. 14. AE energy of different corrosion ratios at increasing speed and fix flow rate.

5.3. Multivariate analysis of variance (MANOVA)

The AE parameters were undertaken as a function of speed, flow rate and corrosion ratios (the averages of all AE parameters results are detailed in Tables A1–A8 in Appendix A). It was hypothesized that there is a significance difference in the variance of all AE parameters when the speed, flow rate and corrosion ratios are changed. In order to verify that, Multivariate Analysis of Variance (MANOVA) was used to obtain the probability value (P value) at a significance level equal to 0.05 as well as to evaluate the change in AE parameters versus the change in the test conditions, which are the corrosion ratio, the speeds and flow rate. Tables 4–6 show the MANOVA results for all AE parameters in all test conditions.

The evaluation of the AE parameters changes under different valve corrosion ratios using MANOVA showed that all AE parameters significantly changed with the change in the corrosion severity, as all the P values are less than 0.05, see Table 4. Likewise,

Table 4
MANOVA of the AE parameters values at overall valve corrosion ratios.

AE Parameters	MS	F	P value
Rise Time	2.87E+08	30.989*	<0.01
Duration	4.97E+08	36.044*	<0.01
Count to Peak	9.48E+05	50.624*	<0.01
Count	2.26E+06	15.685*	<0.01
ASL	2.41E+02	67.216*	<0.01
Amplitude	2.66E+01	61.545*	<0.01
Energy	3.95E+06	15.129*	<0.01
RMS	6.70E−02	41.757*	<0.01

* Significant at 0.05 level.

Table 5
MANOVA of the AE parameters values at different speeds.

Variable	MS	F	P value
Rise Time	4.10E+08	44.149*	<0.01
Duration	8.57E+08	62.087*	<0.01
Count to Peak	1.02E+06	54.217*	<0.01
Count	3.55E+06	24.61*	<0.01
ASL	6.27E+02	174.675*	<0.01
Amplitude	3.17E+01	73.311*	<0.01
Energy	2.67E+07	102.103*	<0.01
RMS	9.10E−02	56.272*	<0.01

* Significant at 0.05 level.

Table 6
MANOVA of the AE parameters values at different flow rates.

Variable	MS	F	P value
Rise Time	7.44E+08	8.021*	0.001
Duration	2.95E+08	21.397*	<0.01
Count to Peak	2.64E+05	14.08*	<0.01
Count	5.53E+05	3.835*	0.028
ASL	1.67E+01	4.658*	0.014
Amplitude	6.51E+00	15.075*	<0.01
Energy	4.93E+06	18.859*	<0.01
RMS	2.00E−03	1.321*	<0.01

* Significant at 0.05 level.

MANOVA was used to evaluate the change in AE parameters under different flow ratios and speeds. Note that all AE parameters are significantly changed, as stated in Table 5. Similar findings were achieved for the change in the AE parameters under different flow ratios, see Table 6. As the P values are smaller than the significance level of 0.05. Therefore, there is a significance difference in the variance of all AE parameters when the speed, flow rate and corrosion ratios are changed.

5.4. Coefficient of variance analysis

The Coefficient of Variance (CV) is a standard measure of dispersion of values, which aims to describe the dispersion of the variable in a way that does not depend on the variable's measurement unit. The CV can be calculated by dividing the standard deviation (SD) by the mean (σ) multiplied by 100 for each of the AE parameters. In this paper, the CV was used to determine the most sensitive AE parameters corresponding to main test variables: valve condition, speed and flow rate. The AE parameter with a high CV value means the parameter values are more useful in fault detection, as it has greater dispersion when the conditions change. In contrast, a parameter with a lower CV value corresponds to smaller dispersion when the conditions change. Then the parameter is less useful in fault detection. See Fig. 16. The CV values of all AE parameters are presented in Table C1 Appendix C.

The bar chart compares the percentage of CV for the AE eight parameters for all the experiments. Significant differences in the percentage of CV are clearly observed among the AE parameters. The RMS has the largest percentage of CV, with a value of 71%, while the rise time and count to peak have the second largest percentages of CV of 66% and 60%, respectively. The value decreased to 54% for count and 44% for duration. The energy, ASL and amplitude have the lowest percentage of CV, with values of 29%, 11% and 2%, respectively. However, the CV percentage of energy remained significantly higher than ASL and amplitude over this ratio frame.

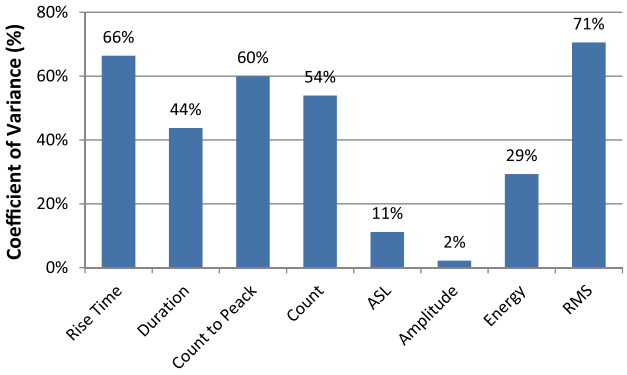

Fig. 16. The coefficient of variance for all the AE parameter.

Consequently, the RMS is considered as the most sensitive parameter to the change of the main variables because it has the greater dispersion when the conditions change, while the amplitude was the least sensitive of all eight parameters to the change in the main test variable.

6. Conclusion

The primary source of the AE signal in the reciprocating compressor was verified using waveform analysis. It was demonstrated that the primary source of the acquired AE signal resulted from the movement of the valve reeds. In addition, all AE parameters values showed a significance changes versus the change in the test conditions (P value is <0.01) as verified using MANOVA. There is a direct relationship between the size of corrosion and the AE parameters; this relationship will be the subject of future investigation. Furthermore, the coefficient of variance results indicates that the RMS with CV = 71% is the best parameter for valve fault detection among all the AE parameters while the ASL and amplitude with values of 11% and 2% respectively have the lowest percentage of CV. It is concluded that the AE signal parameters can be used to detect the valve faults in the reciprocating compressor with the consideration of the variation in the AE parameters sensitivity.

Acknowledgment

The authors would like to extend their greatest gratitude to Institute of Noise and Vibration, University Technology Malaysia for funding the study under HICOE Grant Scheme (PY/2016/06784, PY/2016/07069 & PY/2016/07034) and Fundamental Research Grant Scheme (R.K130000.7840.4F653) financed by the Ministry of Higher Education, Malaysia.

Appendix A

The AE parameters values of all test conditions, emphasizing the sensitivity of AE to corrosion defect progression in varying flow rate and speed conditions is shown in Tables A1–A8 as below:

Table A1
The mean values of the AE rise time for all test conditions.

Valve condition		F1	F2	F3
NC	S1	3406.851	4657.925	5315.836
	S2	14938.85	20639.68	22602.56
	S3	17766.66	22966.16	26,381
	S4	23559.16	24489.26	27502.66
SC	S1	4758.509	4901.211	5692.356
	S2	6532	9557.02	15420.85
	S3	15,716	17859.33	18948.66
	S4	19822.23	21934.26	22358.91
MC	S1	4248.575	4801.315	4968.095
	S2	5005.897	6827.387	7447.692
	S3	6129.664	8565.011	9785.103
	S4	14506.82	15305.44	17339.61
LC	S1	2979.379	3285.803	4507.49
	S2	3648.636	4004.842	8871.116
	S3	6691.042	7522.667	10862.35
	S4	8171.938	9912.697	14528.64
VC	S1	3292.188	3711.347	4332
	S2	3589.769	4112.605	5349.36
	S3	5180.218	7858.936	8495.697
	S4	6341.162	10822.66	12721.56

Table A2
The mean values of the AE Duration for all test conditions.

		F1	F2	F3
NC	S1	13317.56	14951.12	16413.86
	S2	16171.3	25903.5	35286.76
	S3	27936.01	31740.44	39088.4
	S4	35920.49	42121.99	52617.17
SC	S1	14674.18	15150.11	16176.31
	S2	23823.1	26489.49	29709.15
	S3	31586.85	35037.61	37000.44
	S4	33749.01	36,183	39342.02
MC	S1	13294.47	16219.85	19772.1
	S2	16281.19	20083.67	25582.78
	S3	18349.42	26915.35	28512.18
	S4	22404.59	31484.68	33616.84
LC	S1	8906.844	10515.45	10999.02
	S2	16102.73	19553.69	25293.85
	S3	19088.92	21929.39	28969.45
	S4	20046.46	27520.66	30804.85
VC	S1	7427	8287.377	9726.818
	S2	11702.15	12144.82	13360.12
	S3	13028.14	14304.79	16500.61
	S4	15189.98	16658.38	23902.99

Table A3
The mean values of the AE count to peak for all test conditions.

		F1	F2	F3
NC	S1	505.1409	555.0381	629.9041
	S2	568.5128	691.358	884.1923
	S3	832.925	1101.633	1319.941
	S4	1211.858	1437.061	1719.255
SC	S1	316.3818	363.8222	425.9211
	S2	330.6296	435.8776	540.6547
	S3	546.0482	705.94	918.43
	S4	971.9577	1069.726	1263.846
MC	S1	241.1277	333.9057	510.5738
	S2	719.3441	851.0578	891.7089
	S3	896.2524	1093.329	1161.917
	S4	1002.528	1059.379	1206.854
LC	S1	219.5625	249.4082	270.9211
	S2	284.7579	351.9804	383.2316
	S3	313.8571	408.6742	554.8065
	S4	390.3273	509.9335	650.8478
VC	S1	111.6724	127.3934	129.8636
	S2	212.6154	243.615	301.0909
	S3	248.7042	261.7431	446.8103
	S4	333.1094	556.4404	636.62

Table A4
The mean values of the AE count for all test conditions.

		F1	F2	F3
NC	S1	785.2625	910.0733	941.6476
	S2	946.7739	1093.74	1390.923
	S3	1409.174	1732.693	2344.2
	S4	2392.176	3583.701	4209.875
SC	S1	883.7213	910.6604	1042.277
	S2	1498.468	1594.333	1760.939
	S3	1745.406	1816.378	1922
	S4	1816.319	1930.144	1977.831
MC	S1	785.9818	862.5333	897.5263
	S2	826.6296	943.2449	1160.748
	S3	1171.843	1280.16	1438.29
	S4	1630.439	1710.097	1843.141
LC	S1	598.3469	667.5938	795.2895
	S2	1041.579	1143.294	1148.116
	S3	1008.491	1181.174	1476.8
	S4	1238.519	1415.06	1527.82
VC	S1	218.7759	249.303	253.1639
	S2	660.1927	700.155	784.7656
	S3	765.0759	844.3028	952.0423
	S4	856.1923	919.0909	1064.76

Table A5
The mean values of the AE ASL for all test conditions.

		F1	F2	F3
NC	S1	58.65	60.24658	61.28571
	S2	72.9396	74.28409	76.64103
	S3	74.56177	75.19333	78.11892
	S4	75.44595	76.29592	79.01442
SC	S1	53.93878	55.54688	56.78947
	S2	63.5625	64.42202	65.635
	S3	65.21379	67.22535	68.74312
	S4	68.42308	69.63636	70.42
MC	S1	55	56.62295	57.03774
	S2	63.58537	63.89855	63.86893
	S3	65.8481	65.47556	67.15756
	S4	66.1	67.25	68.00484
LC	S1	47.24138	48.63636	47.67213
	S2	59.89474	60.13684	60.88235
	S3	63.4	64.64783	65.55303
	S4	67.5619	68.54032	69.38671
VC	S1	55.78182	56.05263	55.44444
	S2	60.25926	62.30935	60.45918
	S3	64.51282	64.84194	65.43915
	S4	65.56627	65.67633	66.472

Table A6
The mean values of the AE amplitude for all test conditions.

		F1	F2	F3
NC	S1	89.00952	89.50685	90.025
	S2	92.74667	93.12821	94.25
	S3	93.72973	94.59796	95.43624
	S4	95.10481	95.54432	95.94755
SC	S1	89	89.79688	90.98684
	S2	91.07	91.69063	92.0367
	S3	91.53846	91.74545	91.9635
	S4	92.0507	92.36697	93.03103
MC	S1	88.95745	89.39344	89.5283
	S2	89.47561	90.86473	91.24757
	S3	90.51139	91.36667	91.66656
	S4	90.93056	91.5977	92.05085
LC	S1	88.16364	88.63934	89.09474
	S2	88.71579	89.56897	90.15686
	S3	90.30909	90.76957	91.32576
	S4	91.04286	91.27151	91.69486
VC	S1	87.20909	87.64444	88.01579
	S2	88.14815	88.4964	89.93878
	S3	89.73077	90.63548	90.6956
	S4	90.03614	90.92319	91.20106

Table A7
The mean values of the AE energy for all test conditions.

		F1	F2	F3
NC	S1	3064.419	3446.438	4130.55
	S2	4130.66	4601.12	5310.692
	S3	5817.57	6251.341	7320.908
	S4	6996.033	8083.48	8935.256
SC	S1	3609.016	3971.434	4329.319
	S2	4354.476	4844.667	5488.61
	S3	5374.329	5574.213	5825.595
	S4	5658.644	6228.083	6833.622
MC	S1	2860.375	3273.658	3697.918
	S2	3293.516	3417.074	3968.157
	S3	4159.527	4935.439	5404.191
	S4	4689.933	6140.205	6611.661
LC	S1	2641.564	2661.947	2520.311
	S2	2891.407	4174.619	4597.776
	S3	5063.487	5200.826	5507.376
	S4	5496.675	5634.3	5878.24
VC	S1	2502.793	2574.885	2758.394
	S2	4129.813	5018.459	5539.07
	S3	4818.169	5404.422	5823.807
	S4	5078.538	5617.545	5992.07

Table A8
The mean values of the AE RMS for all test conditions.

		F1	F2	F3
NC	S1	0.076315	0.073156	0.065625
	S2	0.198315	0.243127	0.331615
	S3	0.318529	0.367927	0.411182
	S4	0.380859	0.408319	0.439415
SC	S1	0.043078	0.0498	0.03538
	S2	0.109191	0.120598	0.137259
	S3	0.169093	0.177295	0.204208
	S4	0.216469	0.214973	0.241060
MC	S1	0.044338	0.045284	0.043827
	S2	0.069981	0.072133	0.07868
	S3	0.119284	0.124403	0.133912
	S4	0.169466	0.186659	0.190092
LC	S1	0.048698	0.050736	0.039868
	S2	0.108059	0.11115	0.109566
	S3	0.140752	0.133812	0.160609
	S4	0.162967	0.150548	0.177271
VC	S1	0.016259	0.019518	0.017184
	S2	0.076319	0.092793	0.074959
	S3	0.119613	0.124276	0.132193
	S4	0.136022	0.137415	0.148733

Appendix B

The variation of all the AE parameters at increasing flow rate and fix speed are illustrate in Figs. B1–B.8.

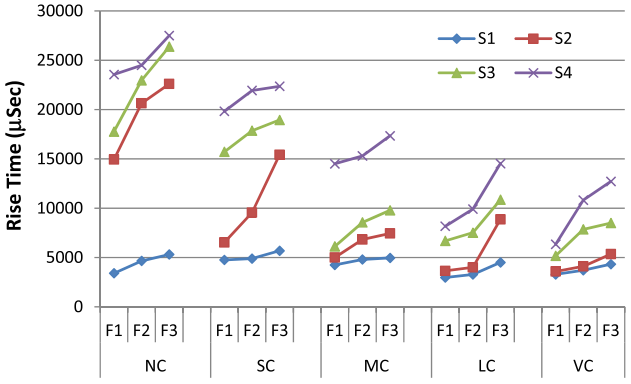

Fig. B1. Rise time of different corrosion ratios at increasing flow rate and fix speed.

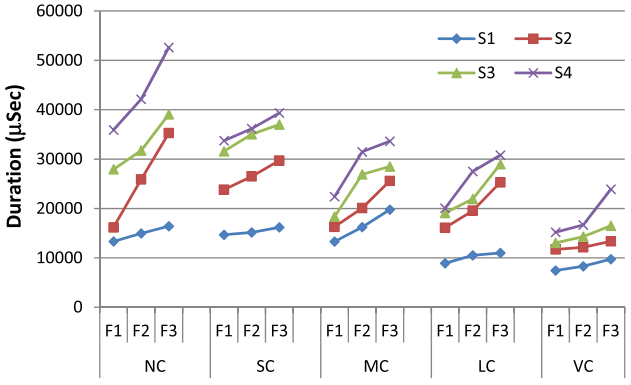

Fig. B2. Duration of different corrosion ratios at increasing flow rate and fix speed.

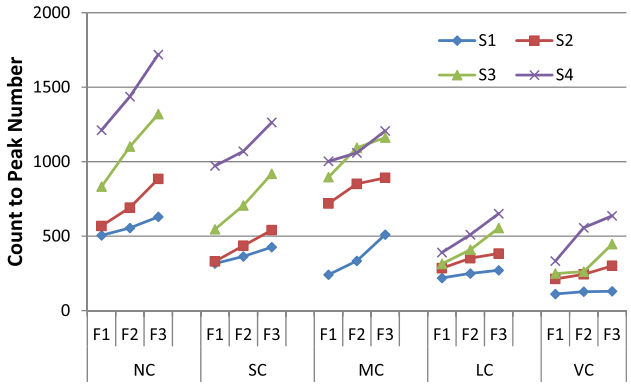

Fig. B3. Count to peak of different corrosion ratios at increasing flow rate and fix speed.

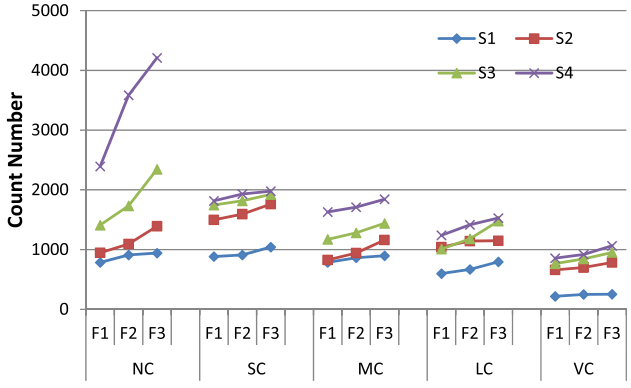

Fig. B4. Counts of different corrosion ratios at increasing flow rate and fix speed.

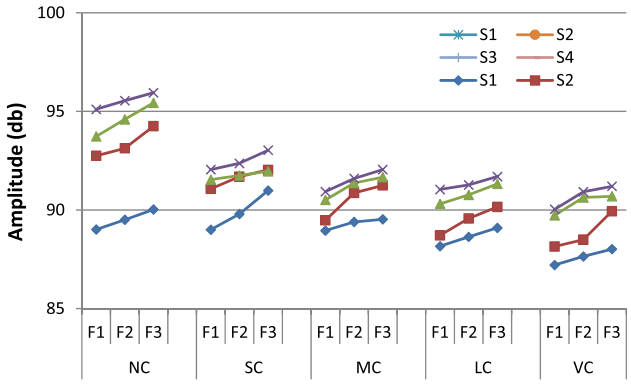

Fig. B5. Amplitude of different corrosion ratios at increasing flow rate and fix speed.

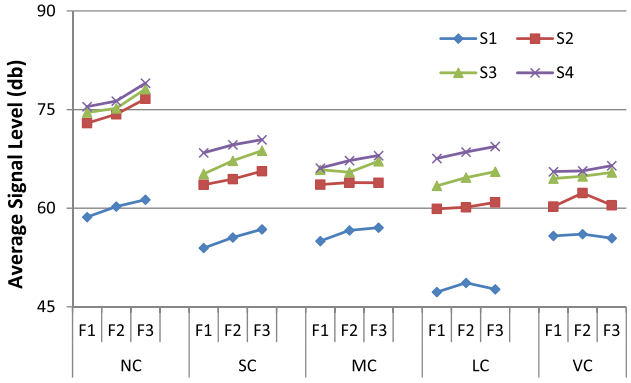

Fig. B6. ASL of different corrosion ratios at increasing flow rate and fix speed.

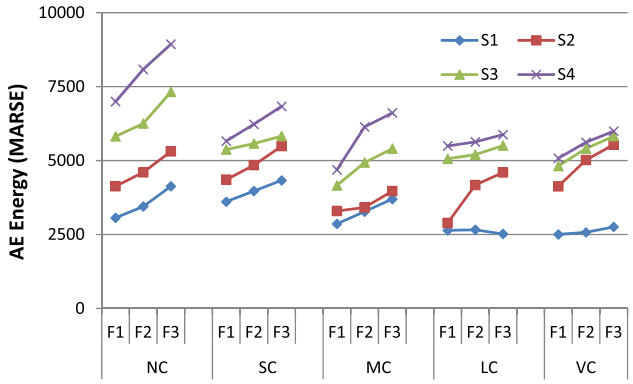

Fig. B7. Energy of different corrosion ratios at increasing flow rate and fix speed.

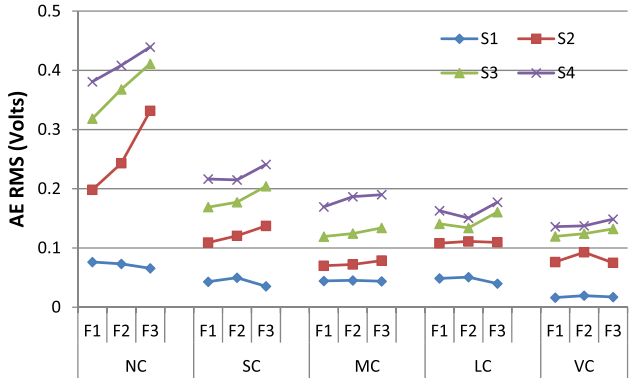

Fig. B8. RMS of different corrosion ratios at increasing flow rate and fix speed.

Appendix C

The mean, standard deviation and coefficient of variance percentage for each AE parameter for all test conditions shown in Table C1.

References

[1] Brown R. Compressors selection and sizing. Houston, USA: Gulf Publishing Company; 2005.
[2] Wang F, Song L, Zhang L, Li H. Fault diagnosis for reciprocating air compressor valve using pV indicator diagram and SVM. In: Proceedings of the Information Science and Engineering (ISISE), 2010 International Symposium on; 2010.
[3] Wang Y, Xue C, Jia X, Peng X. Fault diagnosis of reciprocating compressor valve with the method integrating acoustic emission signal and simulated valve motion. Mech Syst Signal Pr. 2015;56–57:197–212.
[4] Steel JA, Reuben RL. Recent developments in monitoring of engines using acoustic emission. J Strain Anal Eng. 2005;40:45–57.
[5] Al-Obaidi SMA, Leong MS, Hamzah R, Abdelrhman AM. A review of acoustic emission technique for machinery condition monitoring: defects detection & diagnostic. Appl Mech Mater. 2012;229:1476–80.
[6] Ali YH, Rahman RA, Hamzah RIR. Acoustic emission signal analysis and artificial intelligence techniques in machine condition monitoring and fault diagnosis: a review. Jurnal Teknologi. 2014;69:121–6.
[7] Ali YH, Ali SM, Rahman RA, Hamzah RIR. Acoustic Emission and Artificial Intelligent Methods in Condition Monitoring of Rotating Machine – A Review; 2016. p. 212–9.
[8] Vahaviolos SJ. Acoustic emission: standards and technology update. Philadelphia: Astm International; 1999.
[9] Lin Y-H, Liu H-S, Wu C-Y. Automated valve condition classification of a reciprocating compressor with seeded faults: experimentation and validation of classification strategy. Smart Mater Struct. 2009;18:095020.
[10] Ahmed M, Gu F, Ball A. Fault detection of reciprocating compressors using a model from principles component analysis of vibrations. J Phys Conf Ser. 2012;364:012133.
[11] AlThobiani F, Ball A. An approach to fault diagnosis of reciprocating compressor valves using Teager-Kaiser energy operator and deep belief networks. Expert Syst Appl 2014;41:4113–22.
[12] Elhaj M, Gu F, Ball AD, Albarbar A, Al-Qattan M, Naid A. Numerical simulation and experimental study of a two-stage reciprocating compressor for condition monitoring. Mech Syst Signal Pr 2008;22:374–89.
[13] Yang B-S, Hwang W-W, Kim D-J, Tan AC. Condition classification of small reciprocating compressor for refrigerators using artificial neural networks and support vector machines. Mech Syst Signal Pr 2005;19:371–90.
[14] Cui HX, Zhang LB, Kang RY, Lan XY. Research on fault diagnosis for reciprocating compressor valve using information entropy and SVM method. J Loss Prevent Proc 2009;22:864–7.
[15] Shuib Husin D, Hamzah RR. Viability of the Application of Acoustic Emission (AE) Technology for the Process and Management of Maintenance in Industries: Defect Detection, On-Line Condition Monitoring, Diagnostic and Prognostic Tools. In: proceedings of the proceedings of the international multiconference of engineers and computer scientists; 2010.
[16] Ali YH, Omar MH, Rahman RA, Hamzah RIR. Acoustic emission technique in condition monitoring and fault diagnosis of gears and bearings. Int J Acad Res 2014;6.
[17] Salah MSL, Ali M, Al-Obaidi RI Raja, Hamzah Ahmed M, Abdelrhman Mahmoud Danaee. Acoustic emission parameters evaluation in machinery condition monitoring by using the concept of multivariate analysis. ARPN J Eng Appl Sci 2016;11:7507–14.

Table C1
Total of means, stander deviation and coefficient of variation for each AE parameter for all test conditions.

		Rise Time	Duration	Count to Peak	Count	ASL	Amplitude	Energy	RMS
NC	σ	17852.22	29289.05	954.73	1811.69	71.89	93.25	5674.04	0.28
	Sd	8777.00	12441.40	398.17	1117.79	7.34	2.46	1884.74	0.14
	CV	49%	42%	42%	62%	10%	3%	33%	51%
SC	σ	13625.11	28243.44	657.44	1574.87	64.13	91.44	5174.33	0.14
	Sd	6889.41	8926.42	322.66	404.31	5.68	1.11	963.57	0.07
	CV	51%	32%	49%	26%	9%	1%	19%	49%
MC	σ	8744.22	22709.76	830.66	1212.55	63.32	90.63	4370.97	0.11
	Sd	4547.09	6482.83	319.05	369.87	4.52	1.04	1200.59	0.06
	CV	52%	29%	38%	31%	7%	1%	27%	52%
LC	σ	7082.22	19977.61	382.36	1103.51	60.30	90.06	4355.71	0.12
	Sd	3588.11	7359.29	131.63	301.11	8.12	1.20	1321.42	0.05
	CV	51%	37%	34%	27%	13%	1%	30%	41%
VC	σ	6317.29	13519.43	300.81	688.99	61.90	89.39	4604.83	0.09
	Sd	3057.76	4413.83	168.10	291.66	4.21	1.41	1299.07	0.05
	CV	48%	33%	56%	42%	7%	2%	28%	55%
Total	σ	10724.21	22747.86	625.20	1278.32	64.31	90.96	4835.98	0.15
	Sd	7120.45	9950.26	375.14	689.33	7.20	2.00	1418.52	0.10
	CV	66%	44%	60%	54%	11%	2%	29%	71%

[18] Al-Dossary S, Hamzah RIR, Mba D. Acoustic Emission waveform changes for varying seeded defect sizes. Adv Mat Res. 2006;13:427–32.
[19] Al-Ghamd AM, Mba D. A comparative experimental study on the use of acoustic emission and vibration analysis for bearing defect identification and estimation of defect size. Mech Syst Signal Pr 2006;20:1537–71.
[20] Al-Dossary S, Hamzah RIR, Mba D. Observations of changes in acoustic emission waveform for varying seeded defect sizes in a rolling element bearing. Appl Acoust 2009;70:58–81.
[21] Mba D, Hall L. The transmission of acoustic emission across large-scale turbine rotors. Ndt&E Int 2002;35:529–39.
[22] Leahy M, Mba D, Cooper P, Montgomery A, Owen D. Experimental investigation into the capabilities of acoustic emission for the detection of shaft-to-seal rubbing in large power generation turbines: a case study. P I Mech Eng J-J Eng 2006;220:607–15.
[23] El-Ghamry MH, Reuben RL, Steel JA. The development of automated pattern recognition and statistical feature isolation techniques for the diagnosis of reciprocating machinery faults using acoustic emission. Mech Syst Signal Pr 2003;17:805–23.
[24] Gill J, Brown E, Twite M, Horner G, Reuben R, Steel J. Monitoring of a large reciprocating compressor. Proceedings of the COMADEM, 1998.
[25] Kaewwaewnoi W, Prateepasen A, Kaewtrakulpong P. Investigation of the relationship between internal fluid leakage through a valve and the acoustic emission generated from the leakage. Measurement 2010;43:274–82.
[26] Elamin F, Fan YB, Gu FS, Ball A. Diesel engine valve clearance detection using acoustic emission. Adv Mech Eng 2010;2010.
[27] Christian MO, Grosse U. Acoustic emission testing. Heidelberg, Berlin, Germany: Springer-Verlag; 2008.
[28] Mukhopadhyay C, Haneef T, Rao B, Jayakumar T. On-line monitoring of engineering components using acoustic emission technique. Proc Eng 2014;86:496–502.

Dr. Salah M. Ali is currently a research fellow in the Institute of Noise and Vibration - Universiti Teknologi Malaysia (UTM) in Malaysia. He received his B.Sc. (2006) in Mechanical Engineering from University of Technology-Iraq. He obtained his MSc. (2009), and Ph.D (2016) in Mechanical Engineering from University of Malaya and Universiti Teknologi Malaysia respectively. His current research interests include machinery condition monitoring, machinery faults diagnosis and machine learning.

Mr. K.H. Hui is currently a research fellow in Institute of Noise & Vibration, Universiti Teknologi Malaysia. He has an M.Eng.degree in mechanical engineering from the National University of Malaysia. His current research interests include machinery condition monitoring, machinery faults diagnosis, and machine learning.

Dr. L.M. Hee is a Senior Lecturer in the Malaysia-Japan International Institute of Technology, Universiti Teknologi Malaysia. He is currently attached to the Institute of Noise & Vibration as a consultant in the field of vibration analysis and machinery faults diagnosis. He has a Ph.D. in vibration from the Universiti Teknologi Malaysia. His research interests in blade fault diagnosis in turbomachinery. He has over ten years of consultancy experience in machinery diagnostics, structural vibrations and building acoustics in Malaysia.

Dr. M. Salman Leong is a Professor in the Noise & Vibration at the Institute of Noise & Vibration of Universiti Teknologi Malaysia. He has a B.Sc. degree in mechanical engineering and a Ph.D. degree in rotor dynamics from the Heriot-Watt University. His research interest is in vibration analysis and machinery fault diagnostics. He has been involved in industrial consulting since 1984 with prime interests in machinery diagnostics, structural vibrations and building acoustics.

Dr. Ahmed M. Abdelrhman is a Senior Lecturer in School of Engineering-Bahrain Polytechnic in Kingdom of Bahrain. He earned his BSc in Mechanical Engineering from The University of Khartom – Sodan. He obtained his MSc and PhD in Mechanical Engineering at the University of Technology Malaysia. His current research interests include machinery condition monitoring, machinery faults diagnosis, and machine learning.

Dr. Mahdi A. Al-Obaidi is the head of wind energy department at Energy and Renewable Energies Technology Center, University of Technology Baghdad. He earned his BSc in Electrical and Power Engineering from The University of Technology Baghdad 1978. He obtained his MSc from Indian Institute of Technology 1990 and PhD from Damascus University 2013. His current research interests include wind energy, machinery condition monitoring, machinery faults diagnosis, and machine learning.